Revisiting the interaction of heme with hemopexin

Milena Sophie Detzel, Benjamin Franz Schmalohr, Francèl Steinbock, Marie-Thérèse Hopp, Anuradha Ramoji, Ajay Abisheck Paul George, Ute Neugebauer, Diana Imhof

Supplementary material

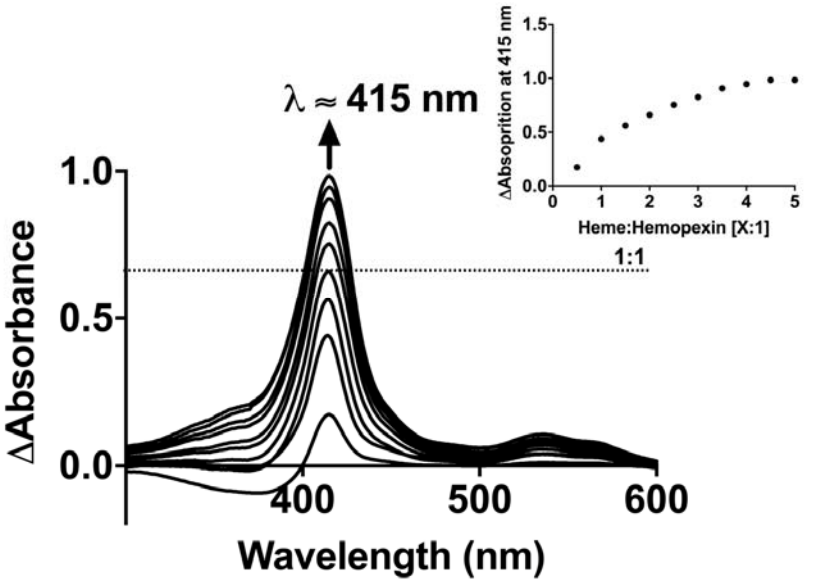

Figure S1: Titration of hemopexin with heme shows an increase in absorbance.
Difference spectra of the heme-hemopexin complex obtained from the interaction of hemopexin (5 µM) with increasing heme concentrations (2.5 – 23.8 µM). Notably, the resulting curve (inset) is not characteristic of a single high-affinity binding site. The absorbance at the Soret band increases at heme:hemopexin ratios exceeding 1:1.

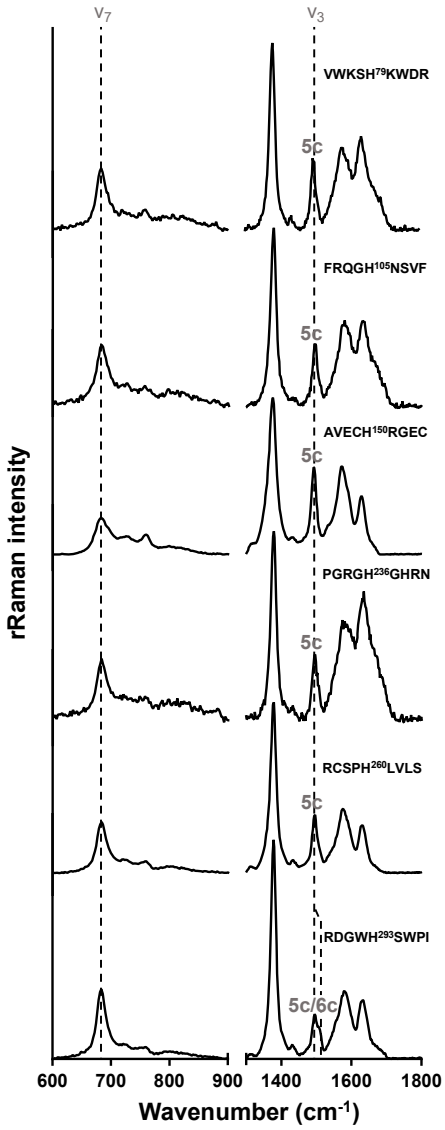

Figure S2: Resonance Raman spectra of heme-peptide complexes.

All complexes were measured at 400 µM in PBS with excitation at 405 nm. As indicated by the ν3-vibrational band, all peptides bound heme in a pentacoordinated fashion, with the exception of peptide motif H293, which showed a mixture of penta- as well as hexacoordination. Peptide H238 could not be measured due to insolubility of the complex.

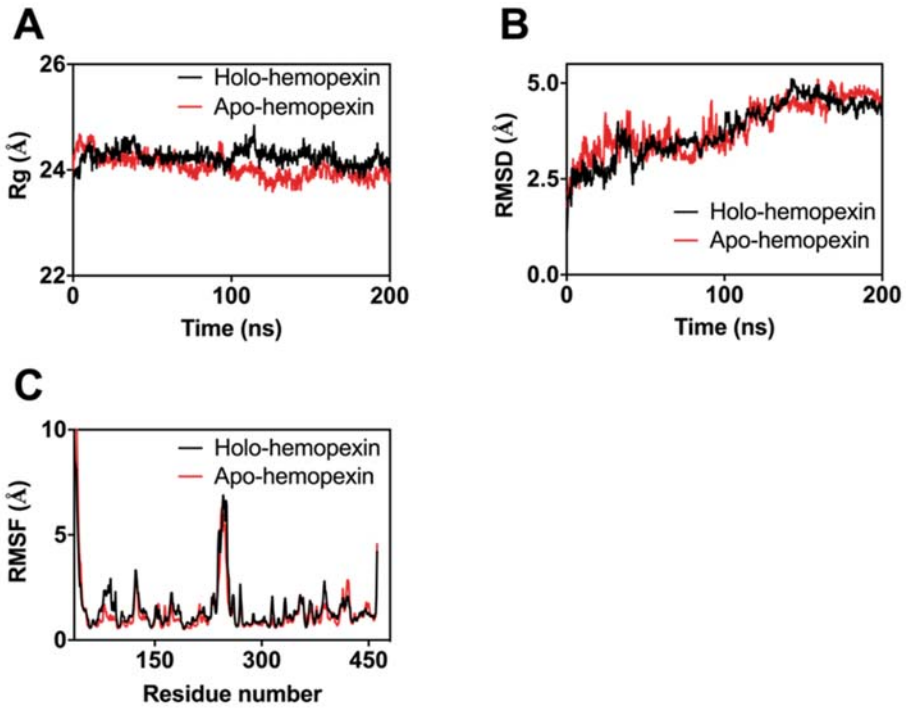

Figure S3: The root-mean-square deviation (RMSD), root-mean-square fluctuation (RMSF), and radius of gyration (Rg) profiles of the apo- and holo-hemopexin models determined from 200 ns long MD simulations.

(A) The backbone RMSD value of apo-hemopexin was calculated as 3.84 ± 0.67 Å with a range of 1.70 Å to 5.16 Å. The backbone RMSD value of holo-hemopexin was calculated as 3.76 ± 0.75 Å with a range of 1.05 Å to 5.27 Å. During both simulations the RMSD values started to stabilize after approximately 170 ns, indicating a stable structure. (B) The Rg values for both, the apo-hemopexin and holo-hemopexin, did not show any significant fluctuations. These slight fluctuations in the overall radius of gyration indicate structural stability during both simulations. Unfolding of the protein structure did not occur. (C) The RMSF values were calculated per residue to elucidate on whether the predictive binding sites do have an influence on the protein's conformation. As expected, significant fluctuations occur at the N-terminal of the protein and to a lesser extent at the C-terminal. The peak patterns between the apo-hemopexin and the holo-hemopexin are similar. This may indicate that having a single heme in the structure does not have a significant impact on either the other heme-binding motifs or on the conformational changes the protein undergoes.

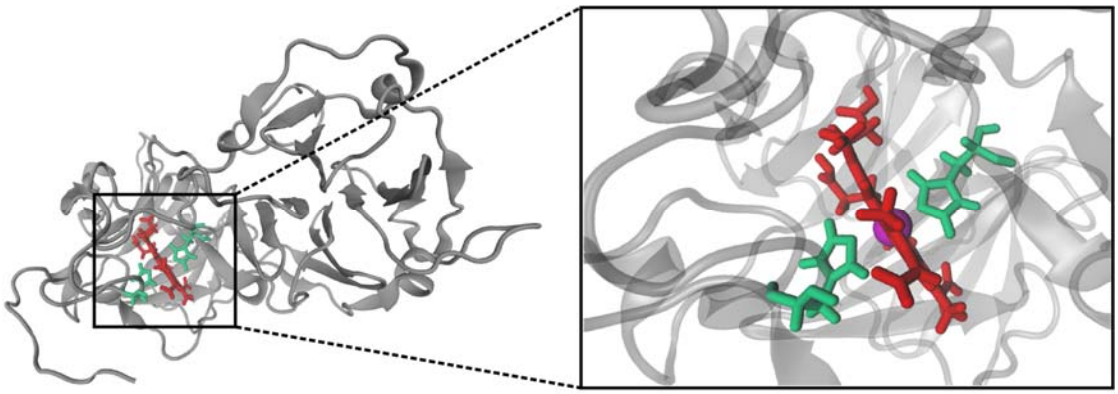

Figure S4: The homology model of human hemopexin accommodates heme in the confirmed binding pocket.

Validation of the homology model (grey ribbons) by docking of heme. Heme (red sticks) docks into the known H236/293 (green sticks) binding pocket observed in the crystal structure, a close-up view of the complex is shown on the right.

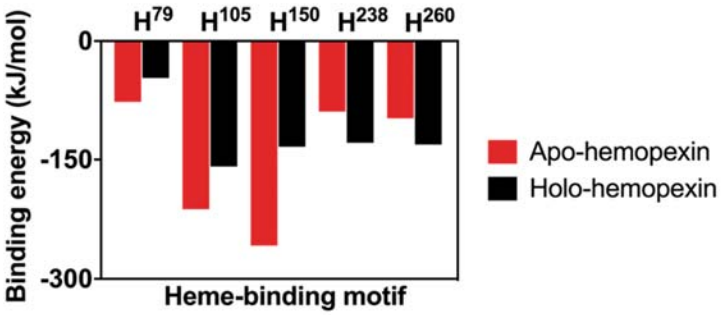

Figure S5: The average binding energy (in kJ/mol) of potential coordinating histidines in both apo- and holo-hemopexin docking complexes.

The binding energy values are obtained from explicit 20 ns MD simulations of the docked complexes in solution that were formed when heme was docked on the specific heme-binding motif of hemopexin. red bars represent apo-hemopexin, black bars represent holo-hemopexin. Heme-binding motifs with higher binding energy values (H79, H238 and H260) indicate stronger binding of heme.

Sequence	K_D [μM]	λ [nm]	Posttrans-lational modification	Disulfide bond	SeqD-HBM	Reference
VWKS**H**^{79}KWDR	3.72 ± 0.23	420	-	-	-*	(Morgan et al., 1993; Satoh et al., 1994)
FRQG**H**^{105}NSVF	0.48 ± 0.24	419	-	-	+	(Paoli et al., 1999)
AVEC**H**^{150}RGEC	n. b.	-	-	C154	-**	(Morgan et al., 1993; Satoh et al., 1994; Paoli et al., 1999)
HRGE**C**^{154}QAEG	n. b.	-	-	C154	+	
PGRG**H**^{236}GHRN	3.61 ± 0.37	421	N-linked at N240	-	+	(Paoli et al., 1999)
RGHG**H**^{238}RNGT	0.35 ± 0.17	420	N-linked at N240	-	+	
GNST**H**^{249}HGPE	n. b.	-	N-linked at N246	-	+	
NSTH**H**^{250}GPEY	n. b.	421	N-linked at N246	-	+	
HGPE**Y**^{254}MRCS	n. b.	-	-	C257	+	
RCSP**H**^{260}LVLS	0.16 ± 0.06	420	-	C257	+	
RDGW**H**^{293}SWPI	5.67 ± 0.58	420	-	-	+	(Paoli et al., 1999)
TKGG**Y**^{335}TLVS	n. b.	-	-	-	+	
VTSLLGCT**H**^{462}	n. b.	-	-	C460	+	
PGRG**H**^{236}GHRNGTGHGNS THHGPEYMRCSP**H**^{260}LVLS ALTSDNHGATYAFSGTHY WRLDTSRDGW**H**^{293}SWPI	1.57 ± 0.32	419	-	C257	+/+/+	(Paoli et al., 1999)

Table S1: Summary of the synthesized peptides.

For the peptides in complex with heme the following properties are given: K_D values, shift of the absorption maximum (λ), posttranslational modifications(Takahashi et al., 1984) and

disulfide bonds(Takahashi et al., 1985) occurring in the protein, prediction by the algorithm SeqD-HBM and reference, where applicable. *This motif was excluded by WESA. **This motif was excluded due to an intramolecular disulfide bond.

Supplementary references

Morgan, W.T., Muster, P., Tatum, F., Kao, S.M., Alam, J., and Smith, A. (1993). Identification of the histidine residues of hemopexin that coordinate with heme-iron and of a receptor-binding region. *J. Biol. Chem.* 268: 6256–6262.

Paoli, M., Anderson, B.F., Baker, H.M., Morgan, W.T., Smith, A., and Baker, E.N. (1999). Crystal structure of hemopexin reveals a novel high-affinity heme site formed between two β-propeller domains. *Nat. Struct. Biol.* 6: 926–931.

Satoh, T., Satoh, H., Iwahara, S.I., Hrkal, Z., Peyton, D.H., and Muller-Eberhard, U. (1994). Roles of heme iron-coordinating histidine residues of human hemopexin expressed in baculovirus-infected insect cells. *Proc. Natl. Acad. Sci. U. S. A.* 91: 8423–8427.

Takahashi, N., Takahashi, Y., and Putnam, F.W. (1984). Structure of human hemopexin: O-glycosyl and N-glycosyl sites and unusual clustering of tryptophan residues. *Proc. Natl. Acad. Sci.* 81: 2021–2025.

Takahashi, N., Takahashi, Y., and Putnam, F.W. (1985). Complete amino acid sequence of human hemopexin, the heme-binding protein of serum. *Proc. Natl. Acad. Sci.* 82: 73–77.